

Fermi Arc in Doped High- $T_c$  CupratesTakashi Yanagisawa<sup>1</sup>, Mitake Miyazaki<sup>1,2</sup> and Kunihiko Yamaji<sup>1</sup><sup>1</sup>Condensed-Matter Physics Group, Nanoelectronics Research Institute, National Institute of Advanced Industrial Science and Technology, Tsukuba Central 2, 1-1-1 Umezono, Tsukuba 305-8568, Japan<sup>2</sup>Department of Physics, Aoyama Gakuin University, 5-10-1 Fuchinobe, Sagamihara, Kanagawa 229-0558, Japan

(Received December 19, 2021)

We propose a  $d$ -density wave induced by the spin-orbit coupling in the  $\text{CuO}$  plane. The spectral function of high-temperature superconductors in the underdoped and lightly doped regions is calculated in order to explain the Fermi arc spectra observed recently by angle-resolved photoemission spectroscopy. We take into account the tilting of  $\text{CuO}$  octahedra as well as the on-site Coulomb repulsive interaction; the tilted octahedra induce the staggered transfer integral between  $p_{x,y}$  orbitals and  $\text{Cu } t_{2g}$  orbitals, and bring about nontrivial effects of spin-orbit coupling for the  $d$  electrons in the  $\text{CuO}$  plane. The spectral weight shows a peak at around  $(\pi/2, \pi/2)$  for light doping and extends around this point forming an arc as the carrier density increases, where the spectra for light doping grow continuously to be the spectra in the optimally doped region. This behavior significantly agrees with that of the angle-resolved photoemission spectroscopy spectra. Furthermore, the spin-orbit term and staggered transfer effectively induce a flux state, a pseudo-gap with time-reversal symmetry breaking. We have a nodal metallic state in the light-doping case since the pseudogap has a  $d_{x^2-y^2}$  symmetry.

KEYWORDS: spectral function, high- $T_c$  cuprate, distortion, spin-orbit coupling, stripes

In recent years, oxide high- $T_c$  superconductors have been investigated intensively; anomalous metallic behaviors as well as high critical temperatures  $T_c$  have been focused in the study of high- $T_c$  cuprates. Clarifying the origin of an anomalous metal with a pseudogap is also a challenging problem attracting many physicists. Recently, a peak crossing the Fermi level in the node direction of the  $d$ -wave gap has been observed in a lightly doped  $\text{La}_{2-x}\text{Sr}_x\text{CuO}_4$  (LSCO) by angle-resolved photoemission spectroscopy (ARPES). The spectral weight shows a peak at around  $(\pi/2, \pi/2)$  for the light-doping case and it extends along the Fermi surface with increasing carrier density.[1,2] The existence of incommensurate correlations has also been reported by neutron-scattering measurements, suggesting vertical stripes in an underdoped region and diagonal stripes in a lightly doped region. Modulation vectors are  $Q_s = (\pi/2, \pi/2)$ ,  $Q_c = (\pi/4, 0)$  (or  $Q_s = (\pi/2, \pi/2)$ ,  $Q_c = (0, \pi/4)$ ) for the hole-doping rate  $x \leq 0.05$ , where  $\pi$  indicates the approximately linear dependence  $\pi = x$ . [3-5]

In the lightly doped region for  $x < 0.05$ , the suggested modulation vector is  $Q_s = (\pi/2, \pi/2)$  and the deviation from the linear dependence exhibits  $\pi < x$ . [4] From the experiments of resistivity in the lightly-doped region of LSCO, the system holds a metallic behavior below  $T_N$ , which may be due to the formation of metallic charge stripes. [6]

The purpose of this paper is to investigate the spectral function of doped high-temperature superconductor in order to elucidate the recently observed ARPES Fermi arc spectra, taking into account the stripe orders suggested by neutron-scattering measurements. We emphasize the importance of distortions of  $\text{CuO}$  octahedra.

The tilting of  $\text{CuO}$  octahedra induces transfer integrals between  $p_{x,y}$  orbitals and  $\text{Cu } t_{2g}$  orbitals, and then the

spin-orbit coupling between  $t_{2g}$  orbitals is not decoupled from  $e_g$  networks. [8,9] For the spin-orbit coupling

$$H_{so} = \lambda \mathbf{s} \cdot \mathbf{p}; \quad (1)$$

matrix elements exist between  $t_{2g}$  orbitals:

$$\langle d_{xz}(r) | H_{so} | d_{yz}(r) \rangle = \lambda \delta_{i, i=2}; \quad (2)$$

$$\langle d_{yz}(r) | H_{so} | d_{xz}(r) \rangle = \lambda \delta_{i, i=2}; \quad (3)$$

$$\langle d_{xz}(r) | H_{so} | d_{yz}(r) \rangle = \lambda \delta_{i, i=2}; \quad (4)$$

$$\langle d_{yz}(r) | H_{so} | d_{xz}(r) \rangle = \lambda \delta_{i, i=2}; \quad (5)$$

We have also matrix elements between  $t_{2g}$  orbitals and  $e_g$  orbitals:

$$\langle d_{xz}(r) | H_{so} | d_{x^2-y^2}(r) \rangle = \lambda \delta_{i, i=2}; \quad (6)$$

$$\langle d_{yz}(r) | H_{so} | d_{x^2-y^2}(r) \rangle = \lambda \delta_{i, i=2}; \quad (7)$$

and those for reversed spins obtained by multiplying by 1. The matrix elements induced by the tilting are

$$h_{px}(x=a/2; y) \langle p_{pd} | d_{xz}(r) \rangle = t_{xz} e^{iQ \cdot r}; \quad (8)$$

$$h_{py}(x; y=a/2) \langle p_{pd} | d_{yz}(r) \rangle = t_{yz} e^{iQ \cdot r}; \quad (9)$$

where  $r = (x; y)$ ,  $Q = (\pi/2, \pi/2)$ ,  $a$  is the lattice constant and  $H_{pd}$  denotes the hybridization term. The factor  $e^{iQ \cdot r}$  induced by the tilting of octahedra in a staggered manner, which leads to the doubled unit cell.  $t_{xz}$  and  $t_{yz}$  are assumed to be given by  $\sin \theta$  for the tilt angle  $\theta$ . In the low-temperature tetragonal (LTT) phase, the spin-orbit coupling may be significantly smaller than that in the low-temperature orthorhombic (LTO) phase, since the integrals between oxygen  $p$  and  $\text{Cu } t_{2g}$  orbitals remain zero along the tilt axis, where oxygen atoms never move:  $t_{yz} = 0$  if the tilt axis is in the  $y$  direction.

The dispersion in the presence of distortions for the  $v$ -band  $p$ - $d$  model is shown in Fig.1. The parameters are as follows:  $d_{x^2-y^2} = 2$ ,  $p = 0$ ,  $d_{xz} = d_{yz} = 1$ ,  $t_{pp} = 0.2$ ,  $t_{xy} = 0.1$ , and  $t_{xz} = t_{yz} = 0.3$  in units of  $t_{pd} = 1$  eV where  $t_{pd}$  is the transfer between  $d$  and  $p$  orbitals and  $t_{pp}$  is that between neighboring oxygen  $p$  orbitals. For the parameters shown above, the splitting at  $X = (\pi; 0)$  is of the order of  $10 \text{ meV} / 100 \text{ K}$ . Each curve is a twofold degeneracy, i.e. Kramers degeneracy as it should be. This structure near the Fermi energy is well understood, using the single-band model with the reduced Brillouin zone, as

$$H_0 = \sum_k \left[ c_k^\dagger c_k + \sum_Q c_k^\dagger c_{k+Q} \right]; \quad (10)$$

where

$$\epsilon_k = 2t(\cos(k_x) + \cos(k_y)) - 4t^0 \cos(k_x) \cos(k_y); \quad (11)$$

and  $Q$  denotes the wave vector  $Q = (\pi; 0)$ .  $c_k$  is a complex parameter satisfying

$$c_{k+Q} = -c_k; \quad (12)$$

$c_k$  is taken as [10,11]

$$c_k = i \sin \left( \frac{1}{2} (2t) Y(k) \right) \quad (13)$$

with  $Y(k) = \cos(k_x) - \cos(k_y)$  in order to reproduce the dispersion for the  $v$ -band CuO model near the Fermi energy, where  $\theta$  is the tilt angle between the Cu-O plane and the Cu-O bond, and  $t^0$  is a constant estimated as  $0.2$ . [11] The dispersion relation of the noninteracting part  $H_0$  in eq. (10) is

$$E_k = \frac{1}{2} \left[ \epsilon_k + \epsilon_{k+Q} \pm \sqrt{(\epsilon_k - \epsilon_{k+Q})^2 + 4J_k^2} \right]; \quad (14)$$

At half-filling, the low-energy excitations are described by the Dirac fermion since there is a Fermi point at  $(\pi; \pi)$ . A light hole doping results in a small Fermi surface around this point with the excitation gap near  $(\pi; 0)$ . This peculiar feature induces a pseudogap in the density of states and we obtain a nodal metallic state. The pseudogap induced by the spin-orbit coupling has a  $d_{x^2-y^2}$  symmetry as apparent from that of  $c_k$ . The density of states for small  $\phi$  shown in Fig.2 clearly indicates a pseudogap structure for a small excitation energy.

The eigenstate of  $H_0$  resembles the  $d$ -density wave proposed for an anomalous metallic state in the underdoped high- $T_c$  cuprates [12], and possesses the following order parameter

$$\psi_{DDW} Y(k) = \hbar c_{k+Q}^\dagger c_k \quad (15)$$

for a real constant  $\psi_{DDW}$ . Although the  $d$ -density wave state appears as a solution of the mean-field equations, this state is hardly stabilized in variational Monte Carlo calculations. Thus, we are motivated to consider the lattice distortion, which is going to stabilize the  $d$ -density wave cooperating with the spin-orbit coupling.

The inhomogeneous ground state under the lattice distortion in the underdoped region has been investigated intensively using the two-dimensional (2D) Hubbard model. [13-16] Within the 2D Hubbard model, the

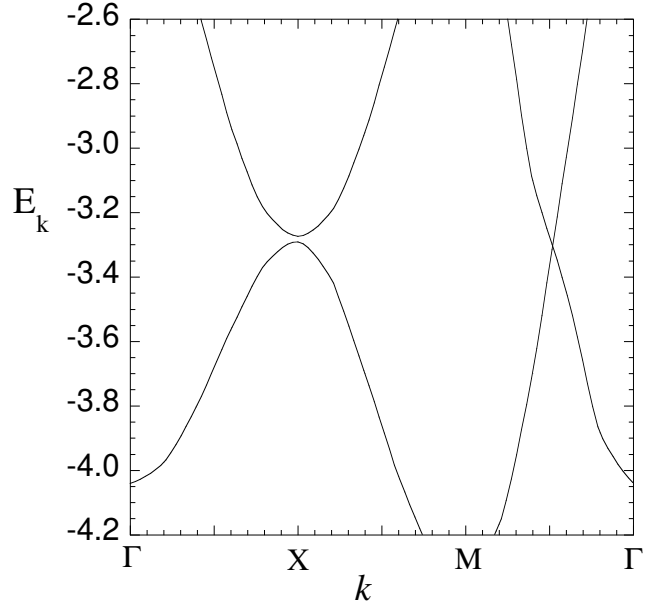


Fig. 1. Dispersion relation for the three-band  $d$ - $p$  model. The parameters are as follows:  $d_{x^2-y^2} = 2$ ,  $p = 2$ ,  $d_{xz} = d_{yz} = 1$ ,  $t_{pp} = 0.2$ ,  $t_{xy} = 0.1$ , and  $t_{xz} = t_{yz} = 0.3$  in units of  $t_{pd}$ , where  $t_{pd}$  is the transfer between  $d$  and  $p$  orbitals and  $t_{pp}$  is that between neighboring oxygen  $p$  orbitals. The splitting at  $X = (\pi; 0)$  is of the order of  $10 \text{ meV}$ . Each curve is a twofold degeneracy, i.e., Kramers degeneracy.

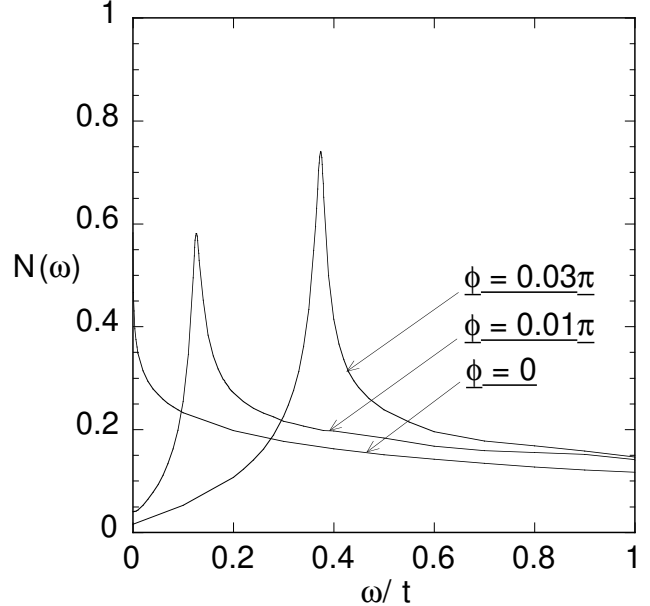


Fig. 2. Density of states for  $\phi = 0, 0.01$  and  $0.03$ . We set  $t^0 = 0$ .

linear dependence of  $\psi$  on  $x$  has been explained by variational Monte Carlo (VMC) methods [16], and furthermore, the saturation of incommensurability for  $x > 0.125$  is also consistent with those obtained by the VMC methods. There is also a tendency towards the formation of stripes under the lattice distortions, with vertical or horizontal hole-rich arrays coexisting with incommensurate magnetism and superconductivity (SC). [7]

We are going to evaluate spectral functions in the

lightly to optimally doped regions. The tilt angle for LSCO is estimated as 14–18° by EXAFS.[17] Thus, is approximately 0.1. If we use 0.2, we have = 0.02. Here, we use a slightly larger value, = 0.05, in actual calculations to obtain sufficient precision because of the numerical difficulty for the small splitting. Clearly, we can expect that this does not change the peculiar feature of the spectra. We determine the variational parameters  $g$  and  $Q_0$  so as to minimize the ground state energy for  $U = 4$  and the carrier density in the range of  $0 < x < 0.2$  by the VMC methods. The Hamiltonian is

$$H = H_0 + U \sum_i n_{i\uparrow} n_{i\downarrow}; \quad (16)$$

where  $H_0$  is given in eq. (1). The wave function is written in a Gutzwiller form:

$$|\Psi\rangle = P_G |\Phi_{MF}\rangle; \quad (17)$$

$P_G$  is the Gutzwiller operator

$$P_G = \prod_i (1 - g) n_{i\uparrow} n_{i\downarrow}; \quad (18)$$

and the mean field wave function  $|\Phi_{MF}\rangle$  is obtained as an eigenfunction of the Hartree-Fock Hamiltonian

$$H_{MF} = H_0 + \sum_i [n_{i\uparrow} \text{sign}(\langle \sigma \rangle) (1 - \langle \sigma \rangle)^{x_{i\uparrow} + y_{i\uparrow}} m_{i\downarrow}] c_{i\downarrow}^\dagger c_i; \quad (19)$$

$n_i$  and  $m_i$  are expressed by the modulation vectors  $Q_s$  and  $Q_c$  for the spin and charge part, respectively.[7] Equivalently, we use the form given by [7,18]

$$n_i = \prod_j \cosh((x_i - x_j^{\text{str}}) = c); \quad (20)$$

and

$$m_i = \prod_j \tanh((x_i - x_j^{\text{str}}) = s); \quad (21)$$

The diagonally striped state has hole arrays in the diagonal direction, while the vertically striped state has hole arrays in the direction parallel to the  $x$  or  $y$  direction. Alternatively, it is also possible to determine the order parameter  $Q_s = \frac{1}{M} \sum_k \langle c_{k+Q_s}^\dagger c_k \rangle$  ( $\sigma = 0, 1$ ;  $M = 1$  or  $2$ ) consistently.[19] We obtain the diagonally striped state for  $x < 0.05$  and the vertically striped state for  $x > 0.05$  as the ground state by the VMC methods.[16] Among the diagonal stripes, the bond-centered striped state is the most stable when we vary the wave function from the site-centered stripe to the bond-centered stripe by the VMC methods. We mention here that the spin-orbit coupling stabilizes the diagonally striped state in the light doping region.[20]

In the evaluations of spectral functions, we consider the effect of  $P_G$  within the mean field theory since we must consider the excited states as well as the ground state. We then evaluate the spectral weight from the eigenvalues  $E_m$  and eigenfunctions  $(u_m)_j$  of the Hamiltonian  $(H_{MF})_{ij}$  in the real-space representation, where  $i$  and  $j$  are site indices. Green's functions are

$$G(i; j; i!) = \sum_m \frac{(u_m)_i (u_m)_j}{i! E_m}; \quad (22)$$

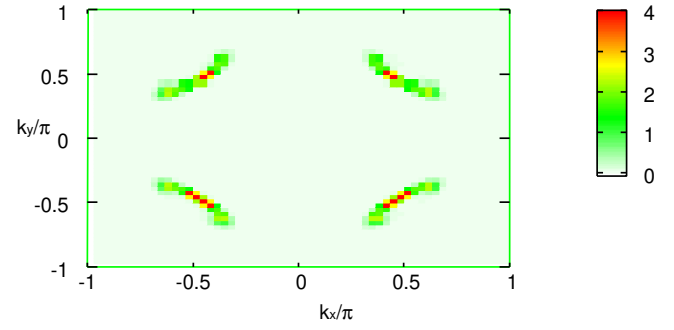


Fig. 3. Contour map of density of states for the diagonally striped state at doping rate  $x = 0.03$  with  $g = 0.05$ ,  $Q_0 = 0.08$ ,  $\sigma = 0$  and  $t^0 = 0.2$ .

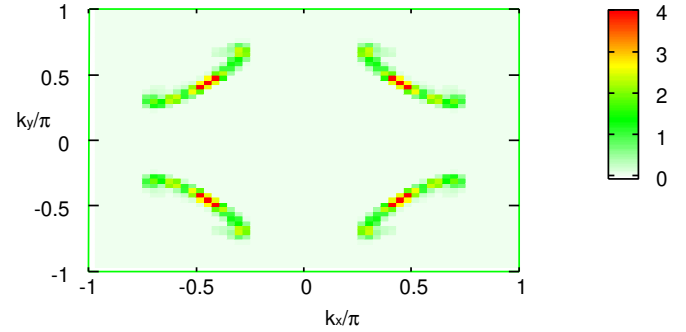


Fig. 4. Density of states at doping rate  $x = 0.0612$  with  $g = 0.05$ . Vertical stripes with a 16-lattice periodicity are assumed.  $Q_0 = 0.10$ ,  $\sigma = 0$  and  $t^0 = 0.2$ .

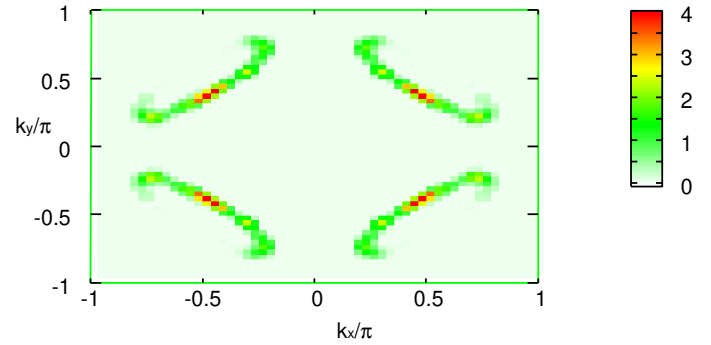


Fig. 5. Density of states at doping rate  $x = 0.125$  with  $g = 0.05$ . Vertical stripes with an 8-lattice periodicity are assumed.  $Q_0 = 0.16$ ,  $\sigma = 0$  and  $t^0 = 0.2$ .

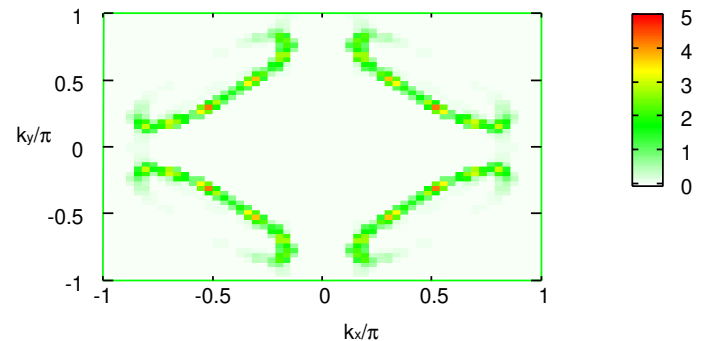


Fig. 6. Density of states for the vertically striped state at doping rate  $x = 0.197$  with  $g = 0.05$ . Vertical stripes with an 8-lattice periodicity are assumed.  $Q_0 = 0.08$ ,  $\sigma = 0$  and  $t^0 = 0.2$ .

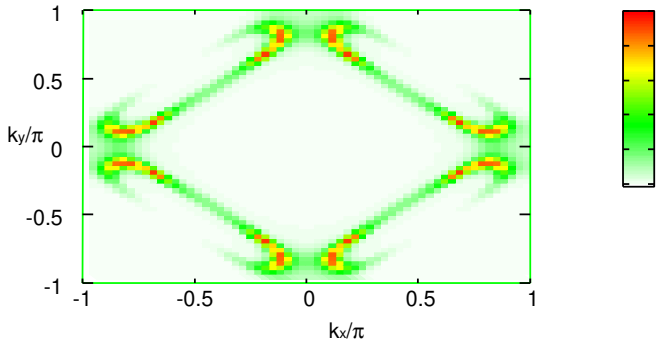


Fig. 7. Density of states for the normal state at doping rate  $x = 0.197$  with  $\beta = 0.05$ ,  $\phi_0 = 0$  and  $t^0 = 0.2$ .

$$g(\mathbf{k}; i!) = \frac{1}{N_a} \sum_{ij} e^{i\mathbf{k} \cdot (\mathbf{R}_i - \mathbf{R}_j)} g(\mathbf{i}; j; i!); \quad (23)$$

where  $N_a$  is the number of atoms. The spectral function is calculated using the formula

$$N(\mathbf{k}; \omega) = \frac{1}{\pi} \text{Im} g(\mathbf{k}; \omega + i0^+); \quad (24)$$

We show the results for  $x = 0.03, 0.061, 0.125$  and  $0.197$  for the parameters obtained by the VMC methods. The contour map of spectra for the light-doping  $x = 0.03$  is shown in Fig. 3 where the calculations were performed on a  $60 \times 60$  lattice for the half-filled diagonal stripes. A peak near  $(\pi/2; \pi/2)$  appears due to the spin-orbit and distortion effects as presented in Fig. 3 for  $\beta = 0.05$ , while it should be noted that the spectra of diagonal stripes without distortion exhibit a one-dimensional structure in the diagonal direction. It has been pointed out that the diagonally striped state can alone explain the opening of the gap if we consider the bond-centered stripe.[21] The spectral functions for  $x = 0.061$  and  $x = 0.125$  with  $\beta = 0.05$  are shown in Figs. 4 and 5, respectively, where we have vertically striped states that have 16-lattice and 8-lattice periodicities, respectively, in accordance with neutron scattering measurements.[4] In Fig. 6 the spectral map at  $x = 0.197$  in the overdoped region is shown, where the stripes have an 8-lattice periodicity. We show the spectra without stripes at  $x = 0.197$  in Fig. 7 for comparison. We observe the absence of spectral weight near  $(\pi/2; 0)$ , which is a characteristic structure originating from the pseudogap. The vertically striped state has one-dimensional-like spectra near  $(\pi/2; 0)$  with the Fermi wave number  $k_F$  corresponding to the one-dimensional quarter-filled band,[13] while the  $k_y$  term contributes to a peak structure at around  $(\pi/2; \pi/2)$ . As a result, we obtain the arc-like spectra for vertical stripes. Thus, as the doping rate  $x$  increases, the spectra near  $(\pi/2; \pi/2)$  in the light-doping case extends towards the 2D-like Fermi surface in the optimally doped region, which occurs as a crossover.

In this paper we have examined novel phenomena stemming from the spin-orbit coupling induced by the tilting of  $\text{CuO}_6$  octahedra. We have shown that the characteristics of the spectral function of doped high- $T_c$  cuprates can be consistently explained using the 2D electronic model with lattice distortions, which is in con-

trast to a theory considering p-orbitals in apical oxygen atoms. [22] We have taken into account the incommensurate structure observed by neutron-scattering experiments. Furthermore, we can expect the following fascinating physics: pseudogap, nodal metal, time-reversal symmetry breaking, diagonal stripes, and string-density wave as a generalization of the d-density wave. In the half-filled case, we obtain a Fermi point, and thus, a peak exists near  $(\pi/2; \pi/2)$  in the density of states that extends to form the Fermi arc spectra as the doping rate increases.[2] In the low-doping case, we obtain a nodal metallic state in the diagonally striped state, since the pseudogap has a  $d_{x^2-y^2}$  symmetry, which is consistent with the experiments of resistivity.[6] The arc is expected to expand with increasing temperature to form the full Fermi surface above the splitting gap  $\sim 100\text{K}$ . [1] Lastly, we comment on a possibility of superconductivity along stripes. The coexistence of superconductivity and stripes has been pointed out for vertical stripes by the VMC methods.[7] It is difficult to have a stable coexistent state of SC and stripes for diagonal stripes in the VMC methods because the SC pairs must have a  $d_{xy}$  symmetry along stripes. Thus, superconductivity is suppressed for light doping.

We are grateful to H. Eisaki for valuable discussions.

- 1) M. R. Norman et al.: Nature 392 (1998) 157.
- 2) T. Yoshida et al.: Phys. Rev. Lett. 91 (2003) 027001.
- 3) J. Tranquada, J.D. Axe, N. Ichikawa, Y. Nakamura, S. Uchida and B. Nandori: Phys. Rev. B 54 (1996) 7489.
- 4) M. Fujita, K. Yamada, H. Hiraka, P.M. Gehring, S.H. Lee, S. Wakimoto and G. Shirane: Phys. Rev. B 65 (2002) 064505.
- 5) M. Matsuda, M. Fujita, K. Yamada, R.J.B. Ingeneau, M.A. Kastner, H. Hiraka, Y. Endoh, S. Wakimoto and G. Shirane: Phys. Rev. B 62 (2000) 9148.
- 6) Y. Ando, A.N. Lavarov, S. Komiyama, K. Segawa and X.F. Sun: Phys. Rev. Lett. 87 (2001) 017001.
- 7) T. Yanagisawa, M. Miyazaki, S. Koikegami, S. Koike and K. Yamaji: Phys. Rev. B 67 (2003) 132408; J. Phys. A 36 (2003) 9337.
- 8) J. Friedel, P. Lenglar and G. Lenman: J. Phys. Chem. Solids 25 (1964) 781.
- 9) K. Yamaji: J. Phys. Soc. Jpn. 57 (1988) 2745.
- 10) N.E. Bonesteel, T.M. Rice and F.C. Zhang: Phys. Rev. Lett. 68 (1992) 2684.
- 11) N.E. Bonesteel: Phys. Rev. B 47 (1993) 9144.
- 12) S. Chakravarty, R.B. Laughlin, D.K. Morr, and C. Nayak: Phys. Rev. B 64 (2001) 094503; Phys. Rev. B 72, 2441 (2003).
- 13) M. Ichio and K. Machida: J. Phys. Soc. Jpn. 68 (1999) 2168; J. Phys. Soc. Jpn. 68 (1999) 4020.
- 14) T. Yanagisawa, S. Koike and K. Yamaji: J. Phys. Condens. Matter 14 (2002) 21; Phys. Rev. B 64 (2001) 184509.
- 15) M. Miyazaki, T. Yanagisawa and K. Yamaji: J. Phys. Chem. Solids 63 (2002) 1403.
- 16) M. Miyazaki, T. Yanagisawa and K. Yamaji: J. Phys. Soc. Jpn. 73 (2004) 1643.
- 17) A. Bianconi et al.: Phys. Rev. Lett. 76 (1996) 3412.
- 18) T. Giamarchi and C. Lhuillier: Phys. Rev. B 42 (1990) 10641.
- 19) E. Kaneshita, M. Ichio and K. Machida: J. Phys. Soc. Jpn. 70 (2001) 866.
- 20) T. Yanagisawa, M. Miyazaki and K. Yamaji: J. Magn. Magn. Mater. 272-276 (2004) 183 (Proceedings of International Conference on Magnetism, Italy, 2003).
- 21) E. Kaneshita, M. Ichio and K. Machida: J. Phys. Soc. Jpn. 72 (2003) 2441.
- 22) H. Kamimura, T. Hamada, H. Ushio: Phys. Rev. B 66 (2002)

054504.